ARTICLE

Structure Characterization of $CuCl_2$-$FeCl_3$-H_2SO_4 Graphite Intercalation Compounds†

Chong-yun Liang, Ren-chao Che, Huan-fang Tian, Hong-long Shi, Jian-qi Li*

Beijing National Laboratory for Condensed Matter Physics, Institute of Physics, Chinese Academy of Sciences, Beijing 100080, China

(Dated: Received on August 30, 2007; Accepted on October 10, 2007)

Graphite intercalation compounds with $CuCl_2$-$FeCl_3$-H_2SO_4 were synthesized via a hydrothermal treatment at 150 °C and exfoliation method. The structure and composition of these graphite intercalation compounds were analyzed by means of X-ray diffraction, energy dispersive X-ray and high-resolution transmission electron microscopy. The results demonstrate that the $CuCl_2$-$FeCl_3$-H_2SO_4 molecules were successfully intercalated into the interlayer of the graphite sheets. The temperature dependence of magnetization was measured from 5 K to 300 K. Two antiferromagnetic transitions of the graphite intercalation compounds were observed at low temperatures. The critical transition temperatures are estimated to be about 50 and 102 K. The related magnetic properties are discussed briefly.

Key words: $CuCl_2$-$FeCl_3$-H_2SO_4, Graphite intercalation compounds, Structure

I. INTRODUCTION

In the past decade, functional materials in nanoscale have received great interest due to their extraordinary structures, electronic and optical properties and their applications in the fabrication of nanodevices [1-3]. In particular, the carbon- or graphite-related nanomaterials attracted great interest. Graphite intercalation compounds (GICs) can be used as the precursors to fabricate new materials in correlation with carbon nanotubes (CNTs) or other CNTs associated nanomaterials. GICs can be prepared by the insertion of exotic atoms or molecules called the intercalated source between the hexagonal two-dimensional sheets of graphite. GICs with transition-metal chlorides are of considerable research interest owing to their attractive magnetic properties, high electrical conductivity, catalytic activity, and the largest flash-heating-induced expansion among GICs. GICs were first synthesized by Schaffautl [4]. These materials often show remarkable ordered structures and significant properties. Possible application potentials of GICs have been proposed in optics, electronics, magnetism, mechanics, battery, electrode materials, chemical catalysis, and catalysis.

Although graphite is a semimetal, the electrons accepted or donated by the intercalant might modify the electronic properties of the pristine graphite system [5-9], which evidently results in a metallic behavior in the GICs. The interlayer conductance of graphite is of 2.5×10^6 s/m [10], but when SbF_5 is intercalated between two-dimensional sheets of graphite, the layer conductance can be enhanced to obtain two orders of magnitude higher than that of graphite [11]. At low temperature, intercalation can stabilize a superconducting state [12] in the as-prepared material. For instance, bulk CaC_6 and YbC_6 materials show notable superconductivity at low temperature and have been extensively studied in recent research [13-18].

To synthesize GICs, several methods such as gas phase technique, vapor transport process, immersion in solution, molten salt method, electrochemical process and aqueous solution synthesis methods are commonly employed [11,14,19-26]. GICs with $FeCl_3$ were synthesized by Rudorf with the zero-gradient method in 1940. Later, a two-zone process was proposed for preparing the single-phase GICs with a tailored stage index [27]. Because two-zone vapor-phase transport process is a time-consuming process, attempts were made to carry out intercalation in solution. Zhu *et al.* reported that GICs with $CuCl_2$-$FeCl_3$-H_2SO_4 can be synthesized via a simple hydrothermal method [28]. This synthesis illustrates a unique way to get a novel GICs with a combination of two different kinds of intercalants such as alkali metal (donor type) and transition-metal chlorides (acceptor type). However, delaminating the layered crystals of GICs with $CuCl_2$-$FeCl_3$-H_2SO_4 into nanosheets has not been carried out, and detailed structure information and physical properties of such material are still lacking.

In this work, two-dimensional crystallites of GICs with $CuCl_2$-$FeCl_3$-H_2SO_4 were synthesized by delaminating layered precursor crystals into nanosheets. These GICs can be regarded as a new type of nanoscale material with a high anisotropy and an ultra-thin thickness. The exfoliated graphite prepared from GICs with $CuCl_2$-$FeCl_3$-H_2SO_4 is potentially attractive as an absorbent. The structure of GICs with

†Part of the special issue from "The 6th China International Conference on Nanoscience and Technology, Chengdu (2007)".

*Author to whom correspondence should be addressed. E-mail: LJQ@aphy.iphy.ac.cn

$CuCl_2$-$FeCl_3$-H_2SO_4 (GICs) was analyzed by a series of techniques, including X-ray diffraction (XRD), high-resolution transmission electron microscope (HRTEM) and Quantum Design MPMS5 SQUID magnetometer. Change of lattice spacing between pure graphite sheets and GICs with $CuCl_2$-$FeCl_3$-H_2SO_4 was carefully examined. Antiferromagnetic transitions at low temperatures of GICs with $CuCl_2$-$FeCl_3$-H_2SO_4 are reported for the first time.

II. EXPERIMENTS

Our GICs were synthesized via a simple hydrothermal process, as described elsewhere [28]. Briefly, high-purity graphite sheets, together with $FeCl_3$, $CuCl_2$, and H_2SO_4 aqueous solution were mixed, stirred and transferred into a Teflon autoclave. Solvents for such a process must possess oxidizing power or contain a dissolved oxidant. In this experiment, 5% of graphite weight of H_2O_2 was used as oxidizer within the system. The process consisted of treating graphite in an appropriate solution for a long time at constant temperature in an inert atmosphere. Then, the container was sealed and heated at 150 °C for 24 h. Therefore, the $FeCl_3$, $CuCl_2$, and H_2SO_4 molecules have enough time to intercalate into the inter-layer spacing of graphite, i.e. along (0002) orientation. Finally, the layered crystals of GICs with $CuCl_2$-$FeCl_3$-H_2SO_4 were delaminated into nanosheets. The XRD for the structure determination of GICs with $CuCl_2$-$FeCl_3$-H_2SO_4 was performed at room temperature on a Rigaku RINT X-ray diffractometer with Cu Kα radiation. energy dispersive X-ray (EDX) microanalysis was done using a Tecnai XL30 SEM. Powder of GICs with $CuCl_2$-$FeCl_3$-H_2SO_4 samples was dispersed in alcohol followed by an ultrasonic treatment. The suspension solution was then dropped onto a holey carbon grid supported by a copper mesh. Electron diffraction and high-resolution transmission electron microscopy analysis were carried out utilizing a Philips CM200/FEG transmission electron microscope equipped with a Gatan imaging filter (GIF). Measurements of the temperature dependence of magnetization were carried out using a superconducting quantum interference device (SQUID MPMS5). Temperature dependence of the DC magnetization was determined with the MPMS5 equipment after cooling the sample from the room temperature down to 5 K in zero field (ZFC). Susceptibility was measured with increasing temperature from 5 K to 300 K.

III. RESULTS AND DISCUSSION

It is well known that during a subsequent intercalation of the three intercalants into the host GICs, different arrangement of three different types of intercalates in the graphite galleries may take place. For example, the formation of GICs starts when the alternating layers of three different intercalants are separated by one or more graphite layers, whereas in the intercalation compounds, two or more different intercalates are together accommodated between two adjacent graphite layers. To determine the structure problem of the arrangement of $CuCl_2$, $FeCl_3$, and H_2SO_4 in graphite lattice, XRD measurements were done. Shown in Fig.1 is a typical XRD pattern recorded from the GICs with $CuCl_2$-$FeCl_3$-H_2SO_4 product. The position and intensity of XRD peaks differ evidently from that of graphite material. The space group of graphite is P63/mmc. Therefore, the XRD data of our GIC differs from the precursor graphite. As marked in Fig.1, (003), (004), (005), and (006) diffraction peaks are indexed well based on a $CuCl_2$-$FeCl_3$-H_2SO_4 intercalated graphite structure, lattice spacing values are 6.67, 4.80, 3.59, and 3.27 Å. Our data is consistent with the data reported [28]. The XRD shows the lack of characteristics of $CuCl_2$ and $FeCl_3$, and the synthesized GICs are shown to be co-intercalated. They contain not only $FeCl_3$ but also $CuCl_2$. Accordingly, $CuCl_2$-$FeCl_3$-H_2SO_4 jointed molecules are successfully intercalated into the interlayer spacing of graphite, leading to the formation of GICs with $CuCl_2$-$FeCl_3$-H_2SO_4. The coexistence of the several different types of compounds in equilibrium may be understood in terms of the Daumas-Herold model [29]. In this model it is assumed that domains of intercalated molecules are present between any graphite layers, and a stage n compound then consist of n different type of domains.

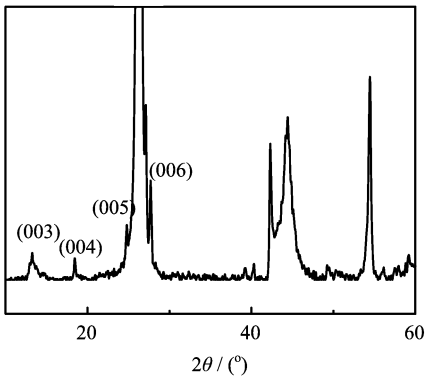

FIG. 1 XRD patterns of the as-synthesized GICs with $CuCl_2$-$FeCl_3$-H_2SO_4.

The possible mechanism for oxidation reaction in which the co-intercalated species $CuCl_2$, $FeCl_3$, and H_2SO_4 are involved can be explained by the following equations:

$$\begin{aligned} &C_{24}{}^{+}(1-u)CuCl_3{}^{-} + (1-v)HSO_4{}^{-} + 2.5H_2SO_4 \\ &\rightarrow C_{24}{}^{+}(1-u)CuSO_4 + (1-v)HSO_4{}^{-} \\ &\quad + (1-u)Cl^{-} + 2(1-u)HCl \cdot (1.5+u)H_2SO_4 \\ &\rightarrow C_{24}{}^{+}[(1-u)CuSO_4 + (2-v-u)HSO_4{}^{-} \\ &\quad + 2(1-u)HCl + (0.5+2u)H_2SO_4] \\ &\quad + (1-u)Cl^{-} + (1-u)H^{+} \end{aligned} \qquad (1)$$

DOI:10.1088/1674-0068/20/06/806-810

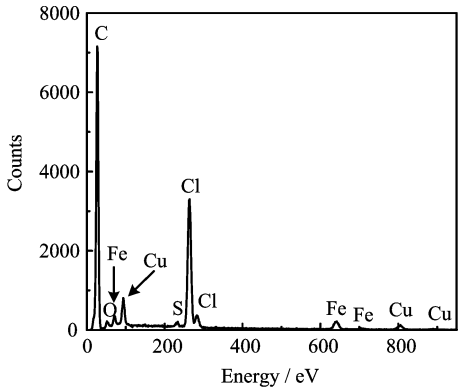

FIG. 2 EDX data of the as-synthesized nanosheets of GICs with $CuCl_2$-$FeCl_3$-H_2SO_4 from SEM-EDX analysis.

$$\begin{aligned} &{C_{24}}^{+}(1-y)FeCl_3{}^{-} + (1-z)HSO_4{}^{-} + 2.5H_2SO_4 \\ &\rightarrow\ {C_{24}}^{+}(1-y)FeSO_4 + (1-z)HSO_4{}^{-} + (1-y)Cl^{-} \\ &\quad + 2(1-y)HCl + (1.5+y)H_2SO_4 \\ &\rightarrow\ {C_{24}}^{+}[(1-y)FeSO_4 + (2-y-z)HSO_4{}^{-} \\ &\quad + 2(1-y)HCl + (0.5+2y)H_2SO_4] \\ &\quad + (1-y)Cl^{-} + (1-y)H^{+} \end{aligned} \tag{2}$$

where, u, v, y, and z are the stoichiometric factors. According to the above discussion, Cl^- are formed, which may take part in the reaction with the surface carbon atoms following the equation below:

$$Cl^- + C \longrightarrow C\text{–}Cl + e^- \tag{3}$$

The compositions of the synthesized material were analyzed by EDX analysis in an FEI XL-30 SEM. A typical EDX spectrum is shown in Fig.2, which displays a broad scan of the material. It is clearly shown that C, Fe, Cu, Cl, S, and O elements are found from the as-prepared samples. These signals result from $FeCl_3$, $CuCl_2$, H_2SO_4, and graphite. To obtain a reliable result, different areas of the GIC specimen were checked and EDX data from the respective areas were compared (the data are not shown here). It is found that the composition is homogeneous all over the sample. It is reasonable to assume that after hydrothermal reaction, the intercalated molecules such as $FeCl_3$, $CuCl_2$, and H_2SO_4 might be decomposed into several types of inorganic ions or groups, i.e. ${SO_4}^{2-}$, Cl^-, ${Fe}^{3+}$, and ${Cu}^{2+}$. All the species of elements might contribute to the EDX signals.

As shown in Fig.3(a), *a*-*b* plane of the GICs with $CuCl_2$-$FeCl_3$-H_2SO_4 does not show obvious difference from that of pure graphite. The hexagonal pattern is due to the electron beam parallel to the *c*-axis of GICs with $CuCl_2$-$FeCl_3$-H_2SO_4 structure. Figure 3(b) illustrates another HRTEM image of the GICs with $CuCl_2$-$FeCl_3$-H_2SO_4 specimen.

To confirm the effects of the intercalated molecules on the GICs with $CuCl_2$-$FeCl_3$-H_2SO_4 structure, we

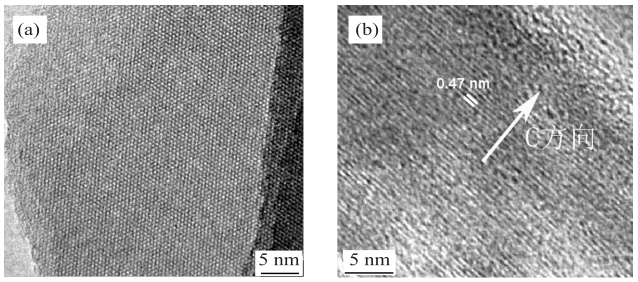

FIG. 3 HRTEM images of nanosheets of GICs with $CuCl_2$-$FeCl_3$-H_2SO_4. (a) *a*-*b* plane of the as-prepared GICs. (b) Electron beam parallel with the a-b planes of the GICs.

tilted the sample along *c*-axis perpendicular to the incident electron beam. As expected, the lattice spacing of (002) planes enlarged to be 0.47 nm, about 0.13 nm more than that of graphite. EELS analysis (not shown here) was performed on the same area and Cu, Cl, Fe elements were found. Therefore, the increase of this lattice spacing is related to the intercalated molecules. To make the spacing value of the HRTEM images useful, we took HRTEM images under a series of defocus values and overfocus values. After a statistical analysis, our distance values of GIC lattice are reliable. In the process of hydrothermal reaction, the inside pressure could reach a rather high point, such as 10 MPa in the sealed container. Therefore, the inorganic molecules had enough energy to intercalate into the hollow spacing of graphite sheets. As to the reason for the formation of GIC nanosheets, after the inorganic molecules move into the spacing of graphite, it is difficult for the graphite to maintain a perfect graphite sheet or plane. That means the graphite sheet can easily become smaller size instead of keeping its original shape. The key factors include the forces resulting both from the high pressure inside the container and from the intercalated molecules.

In ferromagnetic materials the magnetization versus magnetic field relationship exhibits hysteresis. Above a critical temperature, known as the ferromagnetic Curie temperature, the spontaneous magnetization vanishes and the material becomes paramagnetic. Well above the Curie temperature, the susceptibility follows the Curie-Weiss law. The Heisenberg theory of ferromagnetism is based on the assumption that the exchange integral is positive. When the exchange integral is negative, an antiparallel orientation of neighboring spins is favorable, and the specimen has antiferromagnetic nature. In a typical antiferromagnetic material, the most characteristic property of a polycrystalline antiferromagnetic is that its susceptibility shows one or more maximum peaks as a function of temperature, as observed in Fig.4. This characteristic feature may be explained qualitatively on the basis of the following model. Considering a crystal containing two types of atom A and B distributed over two interlocking lattices; for example, let the A atoms occupy the corner point of an

DOI:10.1088/1674-0068/20/06/806-810

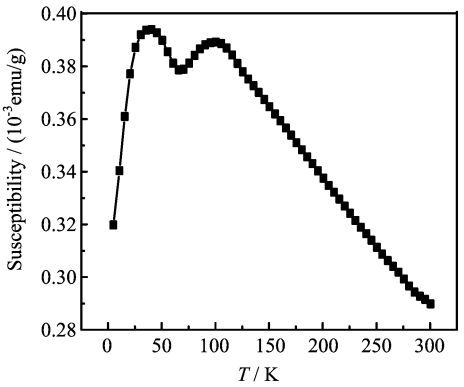

FIG. 4 Zero field cooling magnetic susceptibility curves of nanosheets of GICs with $CuCl_2$-$FeCl_3$-H_2SO_4.

elementary cube, with the B atoms being located at the centers of these cubes. Furthermore, let the interaction between the atoms be such that the A spins tend to line up antiparallel to the B spins. At low temperatures this interaction is very effective and in an external field the resulting magnetization will be small. As the temperature is raised, the efficiency of the interaction becomes less pronounced and the susceptibility increases. Finally, a critical temperature (the Neel temperature) will be reached above which the spins are "free" and above this temperature the antiferromagnetic material becomes paramagnetic decreases with further increase.

It is well known that the intercalate layers are formed of small islands in acceptor GICs [30]. The HRTEM image of GICs with $CuCl_2$-$FeCl_3$-H_2SO_4 shows that similar island structures exist both in the $CuCl_2$ and $FeCl_3$ layers of our system. Figure 4 displays the magnetic susceptibility variation with temperature curves for typical nanosheets of GICs with $CuCl_2$-$FeCl_3$-H_2SO_4 sample under ZFC measurement condition. Pristine graphite should be diamagnetic with a negative value of magnetic susceptibility (10^{-5} order). In contrast, the magnetic susceptibility of nanosheets of GICs with $CuCl_2$-$FeCl_3$-H_2SO_4 was about 100 times that of pristine graphite. The susceptibility of GICs with $CuCl_2$-$FeCl_3$-H_2SO_4 is positive, showing a paramagnetic character at room temperature. At around 47 and 102 K, there are two antiferromagnetic transitions. The convincing evidence is that the slope of the magnetization curve changed from negative value to positive value. Because our GICs with $CuCl_2$-$FeCl_3$-H_2SO_4 product are composed of a ferromagnetic component (graphite) and non-ferromagnetic components. The two critical transition points are partly due to the island nature of $CuCl_2$ and $FeCl_3$ layers.

With the magnetic exception of $CuCl_2$, intercalation reaction from the liquid phase was attempted with the same metal chlorides, to obtain fine natural graphite in which more metal chloride is retained. No intercalation was observed when $AlCl_3$, $BiCl_3$, $AuCl_3$, or $FeCl_3$ were allowed to react.

To investigate the structure and magnetic properties of our GIC products, the data for GIC specimens reported in the previous literature was analyzed and compared with our results, as is discussed carefully below [31-35].

Graphite sheets intercalated with $PdCl_2$ and $NiCl_2$ molecules were confirmed by XRD. Their results showed that the diffraction pattern is different from that of pristine graphite [31]. While stage 2 $CuCl_2$-GICs, obtained by the vapor phase method, and $PdCl_2$-chloroform-GICs and $NiCl_2$-chloroform-GICs were reduced in a gas stream containing 10% of hydrogen at 350 °C [31,32]. Because no magnetic elements are included the system, no obvious magnetic properties is observed.

From the layer sequence of the $FeCl_3$-ICl graphite bi-intercalation compounds (GBCs) with two ICl layers, the degree of the charge transfer is on the order of $FeCl_3$-GIC>ICl-GIC [33]. Various graphite bi-intercalation compounds (GBC) and a graphite multi-intercalation compound (GMC) have been prepared from stage 4 and 5 $FeCl_3$-GIC's, and the lattice dynamics of the resultant GBCs and GMC have been investigated by Raman spectroscopy. The peak frequencies are found to be affected by the bi-intercalated or multi-intercalated species. From this result, the degree of charge transfer was determined to be in the order of IBr, ICl, $SbCl_5$. Multiplier effects on the Raman-active frequencies caused by the bi-intercalated or multi-intercalated species were not observed [34]. The ternary GICs in solutions of $FeCl_3$ in acetyl chloride and in the CH_3COOH-HCl system were synthesized with electrochemical method. The stage 4 and 5 ternary GICs in the former system and stage 3 in the latter were obtained. The identity periods, weight gain, and formation potentials of the synthesized compounds were obtained. The first convincing evidence for the presence of solvent molecules in graphite was found using radiotracer analysis. Thermal analysis results demonstrate that GICs with $FeCl_3$ and ternary GICs with $FeCl_3$ and acetic acid differ markedly in thermal properties [35].

IV. CONCLUSION

Nanosheets of GICs with $CuCl_2$-$FeCl_3$-H_2SO_4 were synthesized by a hydrothermal method and an exfoliation method. The structure of the nanosheets of GICs with $CuCl_2$-$FeCl_3$-H_2SO_4 was comprehensively analyzed by means of XRD and TEM techniques. Evidences of the existence of the intercalated molecules were observed, and the lattice space along *c*-axis direction increased from 0.34 nm to about 0.47 nm. Magnetic susceptibility measurements of nanosheets of GICs with $CuCl_2$-$FeCl_3$-H_2SO_4 reveal that the GICs show a paramagnetic feature above 102 K. This compound shows two clear antiferromagnetic transitions at low temperatures of about 47 and 102 K.

DOI:10.1088/1674-0068/20/06/806-810

V. ACKNOWLEDGMENTS

We would like to thank Mr. W. W. Huang for the assistance in measurements of the temperature dependence of susceptibility and Miss Y. Li for the assistance in preparing samples. This work was supported by the National Natural Science Foundation of China (No.50472044), and the Knowledge Innovation Program of the Chinese Academy of Sciences (No.KJCX2-YW-M04).

[1] R. Martel, T. Schmidt, H. R. Shea, T. Hertel, and P. Avouris, Appl. Phys. Lett. **73**, 2447 (1998).
[2] A. Bachtold, P. Hadley, T. Nakanishi, and C. Dekker, Science **294**, 1317 (2001).
[3] Y. Huang, X. F. Duan, Y. Cui, L. J. Lauhon, K. H. Kim, and C. M. Lieber, Science **294**, 1313 (2001).
[4] P. Schaffautl, J. Prakt. Chem. **21**, 155 (1861).
[5] G. R. Hennig, Prog. Inorg. Chem. **1**, 125 (1959).
[6] W. Rudorff, Adv. Inorg. Chem. 1, 223 (1959).
[7] A. R. Ubbelohde, Proc. R. Soc. A. **309**, 297 (1969).
[8] L. C. F. Blackman, J. F. Mathews, and A. R. Ubbelohde, Proc. R. Soc. A **258**, 339 (1960).
[9] A. R. Ubbelohde, Proc. R. Soc. A **327**, 289 (1969).
[10] M. Dekker, Chem. Phys. Carbon. **8**, 105 (1973).
[11] F. L. Vogel and A. Herold, Mater. Sci. Eng. **31**, 1 (1977).
[12] M. S. Dresselhaus and G. Dresselhaus, Adv. Phys. **51**, 1 (2002).
[13] N. Emery, C. Herold, M. D. Astuto, V. Garcia, Ch. Bellin, J. F. Mareche, P. Lagrange, and G. Loupias, Phys. Rev. Lett. **95**, 087003 (2005).
[14] T. E. Welleri, M. Ellerby, S. S. Saxena, R. P. Smith, and N. T. Skipper, Nature Phys. **1**, 39 (2005).
[15] G. Csanyi, P. B. Littlewood, A. H. Nevidomskyy, C. J. Pickard, and B. D. Simons, Nature Phys. **1**, 42 (2005).
[16] N. Emery, C. Herold, and P. Lagrangea, J. Solid State Chem. **178**, 2947 (2005).
[17] M. Calandra and F. Mauri, Phys. Rev. Lett. **95**, 237002 (2005).
[18] I. I. Mazin and S. L. Molodtsov, Phys. Rev. B **72**, 172504 (2005).
[19] M. S. Dresselhaus and F. Dresselhaus, Adv. Phys. **30**, 139 (1981).
[20] J. S. Gao, C. L. Xin, and L. Yao, *Gao Jishu Xin Cailiao*, Beijing: China Science and Technology Press, 676 (1993).
[21] J. M. Skowronski, Carbon **24**, 185 (1986).
[22] M. S. Dresselhaus and G. Dresselhaus, Adv. Phys. **51**, 1 (2002).
[23] F. Kang, Y. Leng, T. Y. Zhang, and B. Li, Carbon **36**, 383 (1998).
[24] M. Inagaki, J. Mater. Res. **4**, 1560 (1989).
[25] M. S. Dresselhaus, *Intercalation in Layered Materials*, New York: Plenum, (1986).
[26] P. Scharff, E. Stumpp, and C. Ehrhardt, Synth. Met. **34**, 121 (1989).
[27] L. B. Ebert, Annu. Rev. Mater. Sci. **6**, 181 (1976).
[28] J. P. Zhu, Z. Y. Chen, and C. S. Wang, Mater. Lett. **57**, 2145 (2003).
[29] N. Daumas and A. Herold, C. R. Acad. Sci. C **268**, 273 (1969).
[30] T. Enoki, M. Suzuki, and M. Endo, *Graphite Intercalation Compounds and Applications*, Oxford: Oxford University Press, 236 (2003).
[31] H. Shioyama, Y. Yamada, A. Ueda, and T. Kobayashi, Carbon. **43**, 2374 (2005).
[32] T. Abe, Y. Yokota, Y. Mizutani, M. Asano, T. Harada, M. Inaba, and Z. Ogumi, J. Mater. Res. **11**, 3039 (1996).
[33] T. Abe, Y. Yokota, Y. Mizutani, M. Asano, and T. Harada, Phys. Rev. B **52**, 14159 (1995).
[34] T. Abe, M. Inaba, Z. Ogumi, Y. Yokota, and Y. Mizutani, Phys. Rev. B **61**, 11344 (2000).
[35] A. V. Dunaev, N. E. Sorokina, N. V. Maksimova, and V. V. Avdeev, Norganic Materials **41**, 127 (2005).

DOI:10.1088/1674-0068/20/06/806-810